

Low-power total reflection X-ray fluorescence spectrometer using diffractometer guide rail

Ying Liu,^{a)} Susumu Imashuku, and Jun Kawai

Department of Materials Science and Engineering, Kyoto University, Yoshida Honmachi, Sakyo-ku, Kyoto 606-8501, Japan

(Received 21 June 2013; accepted 31 August 2014)

An X-ray diffractometer (XRD) was modified to a low-power total reflection X-ray fluorescence (TXRF) spectrometer. This was realized by reducing the XRD tube power (3 kW) down to 10 W by a Spellman power supply. The present spectrometer consisted of a waveguide slit, Si-PIN detector, a goniometer and two Z-axis stages that were set on a diffractometer guide rail. This unit was easy in assembly. The first measurements with this spectrometer were presented. The minimum detection limit for Cr was estimated to be a few nanograms or at the level of 10^{13} atoms cm^{-2} . © 2014 International Centre for Diffraction Data. [doi:10.1017/S0885715614000797]

Key words: low-power TXRF, high-power XRD tube, power supply, diffractometer guide rail

I. INTRODUCTION

In total reflection X-ray fluorescence (TXRF) spectrometry, monochromatic X-rays from high-power X-ray sources (kW X-ray tube or synchrotron radiation) are generally used for the detection of trace and ultra-trace elements (Klockenkämper, 1997; Wobrauschek, 2007; Strelu *et al.*, 2008). Using monochromatized synchrotron radiation (SR) for the TXRF analysis has made it possible to detect elements in the femtogram (10^{-15} g) range. However, such low detection limits were only achieved for several elements in Si wafer analysis (Wobrauschek *et al.*, 1997; Sakurai *et al.*, 2002; Strelu *et al.*, 2006). In addition, the limited access to SR facility restricts its practical applications in semiconductor industry. On the other hand, Kunimura and Kawai (2007) have developed a portable TXRF spectrometer with a 1 W X-ray tube, and found that when low-power X-ray tube was used, non-monochromatic TXRF was more sensitive than monochromatic TXRF. The lowest detection limit of 10 picogram (pg) achieved by the portable TXRF (Kunimura and Kawai, 2010a) was only four orders of magnitude higher compared with that obtained by an SR-TXRF spectrometer. The portable TXRF spectrometer has been proved a versatile tool by which many analytical problems could be solved (Kunimura and Kawai, 2010a; Liu *et al.*, 2013). Accordingly, the low-power TXRF technique without incident beam monochromatization is rapidly becoming an alternative method in TXRF spectrometry to efficiently perform rapid multi-elemental determination at low cost. At the same time, realization of the non-monochromatic and low-power TXRF analysis is severely limited to the laboratory that has an appropriate X-ray source – a specially designed X-ray tube for low-power load (<10 W). This limitation might be reduced if a high-power X-ray source existing in a widely used laboratory instrument, such as X-ray diffractometer (XRD), could be switched its use to low-power TXRF analysis. The application of XRD tube in high-power TXRF analysis has been reported previously (Wobrauschek

and Kregsamer, 1989; Greaves *et al.*, 1995; Wobrauschek *et al.*, 2008). For instance, Wobrauschek and Kregsamer (1989) developed a compact unit (WOBI-module) carrying all necessary components for high-power TXRF analysis that can be attached to the tube housing for the XRD tube. In contrast to the application of the XRD tube in high-power TXRF analysis, in the present report, with the aim to explore the suitability of high-power XRD tube to low-power TXRF analysis, we modified an XRD to a low-power TXRF spectrometer by reducing the XRD tube power (3 kW) down to 10 W by a power supply.

II. EXPERIMENTAL

Schematic of the low-power TXRF spectrometer setup is presented in Figure 1. The setup comprised an XRD tube, a power supply, a water-cooling unit, a waveguide slit, a goniometer, two Z-axis stages, a diffractometer guide rail, and an X-ray detector. Apart from the power supply and water-cooling unit, all the other elements were contained in a box with the size of 40 cm (height) × 40 cm (width) × 45 cm (length). A Mo-target X-ray tube (PW2275/20, Philips, the Netherlands) that originally used in an XRD (XD-3A, Shimadzu, Japan) was employed as an excitation source. Four Be windows (300 μm) allowed simple changeover from line to point focus and vice versa in this tube. In this setup, one Be window through which the X-rays emerged with a line focus of 0.4 × 12 mm was used. The anode design of the XRD tube was capable to power loads up to 3 kW (60 kV max. and 50 mA max.). However, the tube was reduced its power down to 10 W by a Spellman power supply (30 kV max. and 10 mA max., Model: DXM30*300, Spellman, USA). A standard shielded RS-232 cable was used to connect the power supply to the serial port on a standard personal computer. Remote programming and monitoring the output voltage and current were allowed via RS 232 interface of the power supply. A simple water-cooling unit consisting of a magnetic drive centrifugal pump (MD-6, Iwaki, Japan) was made for the tube cooling. The maximum operating pressure of this pump is 0.02 MPa. The maximum flow obtained at

^{a)} Author to whom correspondence should be addressed. Electronic mail: liu.ying.48r@st.kyoto-u.ac.jp

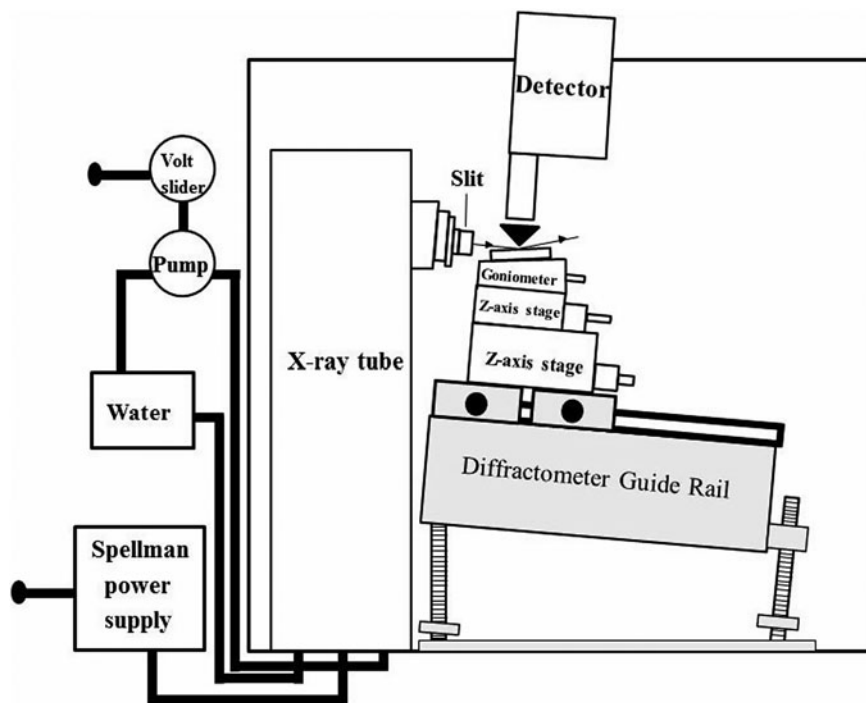


Figure 1. Schematic view of the low-power TXRF spectrometer setup in the incident plane (not to scale).

zero discharge head is $8\text{--}9\text{ Liters min}^{-1}$. A waveguide slit proposed by Egorov and Egorov (2004) was placed in front of the X-ray exit window of the tube housing (Figure 2). This slit was capable to restrict the continuum X-rays from the tube to a parallel beam of 10 mm in width, 10 or 20 μm in height. Goniometer as well as two Z-axis stages was set on a diffractometer guide rail (Rigaku-Denki, Japan). In experiments, the sample holder was put on top of the goniometer. The angle between the incident beam and the surface of the sample holder was manually adjusted via the goniometer. Vertical position of the sample carrier was manually adjusted via the Z-axis stages. The supporting plane of the guide rail was made to tilt by an angle of 6° with respect to the horizontal plane, with the aim of permitting the sample stage parallel to the primary beam at a takeoff angle of 6° . The detector in use is Peltier-cooled Si-PIN photodiode detector (X-123, Amptek, USA) with an effective detection area of 7 mm^2 and silicon thickness of $300\ \mu\text{m}$. This detector unit contained a preamplifier and a digital signal processor in the detector housing and was directly connected to a computer via a USB cable.

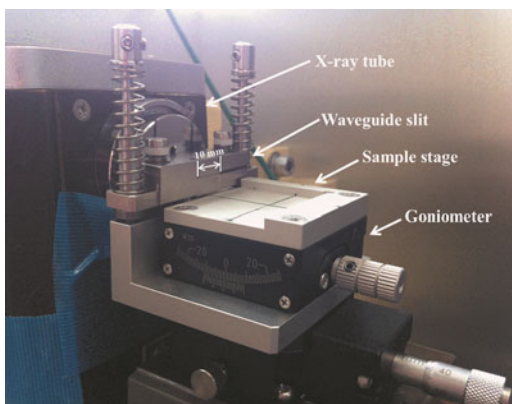


Figure 2. (Color online) Photograph of the waveguide slit.

III. RESULTS AND DISCUSSION

Figure 3 shows two TXRF spectra of a blank quartz glass optical flat ($\lambda/20$ of surface flatness, $\lambda = 632.8\text{ nm}$, Sigma Koki, Japan) measured at 20 kV, 0.5 mA and 10 kV, 1.0 mA, respectively. The scattered X-ray spectra were measured with the aim to estimate the spectral distribution of the primary X-rays. In both spectra, SiK-line, MoL α and L β lines and ArK-line were detected. Ar and Si were detected due of air containing 0.93% Ar and the quartz optical flat. At the voltage of 20 kV, the Si peak was higher than that at 10 kV. This is because of the fact that a thicker layer in the optical flat was passed through when the X-ray tube was operated at 20 kV since the penetration depth of the beam into the optical flat increased with X-ray photon energy increment. Mo L-characteristic X-rays were detected because of the anode material of the X-ray tube. MoL γ lines could not be seen in the spectra because they were overlapped with the strong

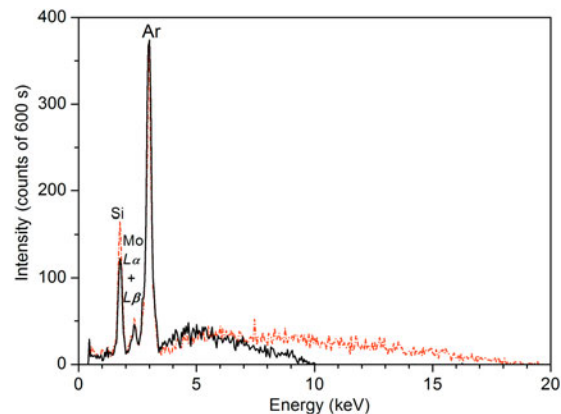


Figure 3. (Color online) TXRF spectra for a blank quartz glass optical flat measured at the X-ray generator power of 10 W. The dashed and dotted line was measured at 20 kV and 0.5 mA, the solid line was measured at 10 kV and 1.0 mA.

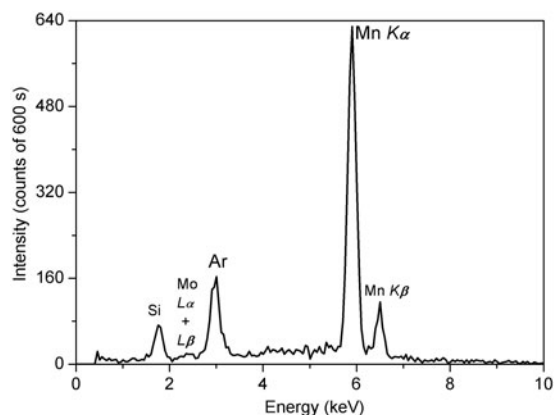


Figure 4. TXRF spectrum for a dry residue containing 2 µg Mn. X-ray tube was operated at 10 kV and 1.0 mA.

ArK-lines. Bremsstrahlung edge energy in each spectrum agreed well with the maximum energy of the X-ray photons at the corresponding accelerated voltage.

Figure 4 shows the TXRF spectrum of a dry residue containing 2 µg Mn measured at 10 kV and 1.0 mA. This sample was prepared by dropping a 2-µl portion of a 1000 ppm Mn standard solution (Wako Pure Chemical Industries, Japan) onto the quartz optical flat and then dried on a heater. Si, Mo, and Ar peaks were detected because of the same reasons as those explained above. Both MnK α and K β lines from the sample residue were detected. The ratio of MnK α /K β intensity was 150:17, which agreed well with the theoretical value (Kortright and Thompson, 2009). The minimum detection limit (MDL) for Mn evaluated from the following equation was 35 ng:

$$\text{MDL} = 3m \frac{\sqrt{(I_B/t)}}{I_N} \quad (1)$$

where m is the sample amount (ng), I_N and I_B are the net and background intensity (counts/s), respectively, and t is the measurement time (s).

Figure 5 shows the TXRF spectra for a dry residue containing 1 µg Cr measured at the glancing angles of 0.1° and 0.3°. The applied voltage was 10 kV and the electron current was 1.0 mA. Chromium was detected in both spectra. The

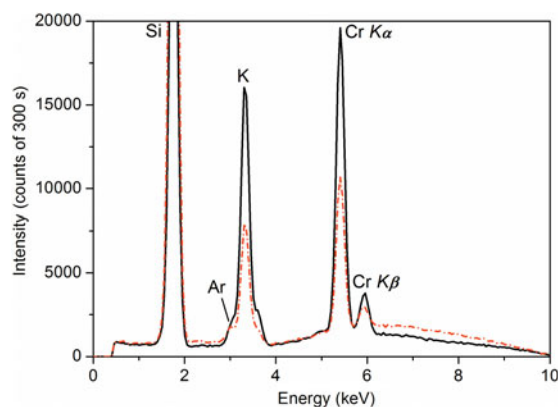


Figure 5. (Color online) TXRF spectra for a dry residue containing 1 µg Cr measured at the glancing angles of 0.1° (solid) and 0.3° (dashed and dotted). X-ray tube was operated at 10 kV and 1.0 mA.

potassium peaks were also detected because the Cr dry residue was obtained by pipetting 1-µl portion of a 1000 ppm Cr standard solution for atomic absorption (K₂Cr₂O₇ in 0.015 mol l⁻¹ HNO₃) (Nacalai Tesque, Japan) onto the quartz optical flat. Argon peaks were strongly overlapped with the potassium peaks. The signal-to-background ratios of the CrK α and K β peaks at the glancing angle of 0.1° were two times higher than those at 0.3°. At the angle of 0.1°, the net and background intensities of the CrK α peak were 263 and 60 counts s⁻¹, respectively. The MDL for Cr was estimated to be 5 ng. This was equivalent to 200 ppb Cr in 25 µl of solution, or the level of 10¹³ atoms cm⁻² if the irradiated area on the optical flat was assumed to be 1 cm². The MDL for Cr (5 ng) was 1/7 of that for Mn (35 ng); this might be attributed to the following reasons: (1) a waveguide slit with the height of 20 µm was used for Cr measurement, compared with 10 µm in Mn measurement. Owing to the fact that the incident beam intensity formed by the waveguide slit increased as the increase of the slit height if slit height exceeds 3 µm (Egorov and Egorov, 2004), when the waveguide slit with the height of 20 µm was used more X-ray photons excited the Cr-containing dry residue; (2) the fluorescent X-rays of Cr were fully recorded since a smaller size dry residue was formed on the optical flat in Cr analysis (sample volume used in Cr analysis was 1/2 of that of Mn). The MDL for Cr (5 ng) was comparable with that obtained by the portable TXRF spectrometer with a commercial low-power X-ray tube of 1 W (Kunimura and Kawai, 2007), while it was two orders of magnitude higher than that obtained by the portable TXRF spectrometer with a commercial low-power X-ray tube of 5 W (Kunimura and Kawai, 2010b). It should be noted that the 5 ng MDL for Cr was achieved by the basic setting of this spectrometer without optimization with respect to the geometry and the experimental conditions. The detection sensitivity of the spectrometer would be increased via the optimization.

IV. CONCLUSIONS

From the hint brought up by the WOBI-module using existing X-ray tube and X-ray generator for high-power TXRF analysis (Wobruschek and Kregsamer, 1989; Wobruschek *et al.*, 2008), we designed and constructed a low-power TXRF spectrometer from the modification of an XRD. The WOBI-module mechanically attached to an XRD tube housing by screws was mainly composed of a slit collimation system, a cut-off reflector or multilayer monochromator, and a sample holder device. A monochromator was necessary in this module because of the high-power (kW) operation of the XRD tube. In the present TXRF spectrometer, the XRD tube was reduced its power (3 kW) down to 10 W by a Spellman power supply. Since non-monochromatic X-rays were applied to sample excitation, a monochromator was not needed. The TXRF spectrometer was easy in arrangement and low in running cost. The suitability of high-power XRD tube in low-power TXRF analysis has been proven via the spectrometer. The MDL achieved for Cr was a few nanograms or at the level of 10¹³ atoms cm⁻². The initial results are promising. Optimization of the geometry and experimental conditions should be conducted to enhance the performance of the spectrometer.

ACKNOWLEDGEMENT

The authors highly acknowledge the work of Professor Peter Wobrauschek (Atominstytut, TU WIEN, Austria) for giving a good hint to our study.

- Egorov, V. K. and Egorov, E. V. (2004). "The experimental background and the model description for the waveguide-resonance propagation for X-ray radiation through a planar narrow extended slit," *Spectrochim. Acta B* **59**, 1049–1069.
- Greaves, E. D., Meitín, J., Sajo-Bohus, L., Castelli, C., Liendo, J., and Borger, M. D. C. (1995). "Trace element determination in amniotic fluid by total reflection X-ray fluorescence," *Adv. X-Ray Chem. Anal. Jpn.* **26s**, 47–52.
- Klockenkämper, R. (1997). *Total Reflection X-ray Fluorescence Analysis* (Wiley, New York).
- Kortright, J. B. and Thompson, A. C. (2009). "X-Ray Emission Energies," in *X-ray Data Booklet*, edited by A. C. Thompson (Lawrence Berkeley National Laboratory, Berkeley), 3rd ed., pp. 1–19 and 1–20.
- Kunimura, S. and Kawai, J. (2007). "Portable total reflection X-ray fluorescence spectrometer for nanogram Cr detection limit," *Anal. Chem.* **79**, 2593–2595.
- Kunimura, S. and Kawai, J. (2010a). "Portable total reflection X-ray fluorescence spectrometer for ultra trace elemental determination," *Adv. X-Ray Chem. Anal., Jpn.* **41**, 29–44.
- Kunimura, S. and Kawai, J. (2010b). "Polychromatic excitation improves detection limits in total reflection X-ray fluorescence analysis compared with monochromatic excitation," *Analyst* **135**, 1909–1911.
- Liu, Y., Imashuku, S., and Kawai, J. (2013). "Multi-element analysis by portable total reflection X-ray fluorescence spectrometer," *Anal. Sci.* **29**, 793–797.
- Sakurai, K., Eba, H., Inoue, K., and Yagi, N. (2002). "Wavelength-dispersive total-reflection X-ray fluorescence with an efficient Johansson spectrometer and an undulator X-ray source: detection of 10^{-16} g-level trace metals," *Anal. Chem.* **74**, 4532–4535.
- Streli, C., Pepponi, G., Wobrauschek, P., Jokubonis, C., Falkenberg, G., Záray, G., Broekaert, J., Fittschen, U., and Peschel, B. (2006). "Recent results of synchrotron radiation induced total reflection X-ray fluorescence analysis at HASYLAB, beamline L," *Spectrochim. Acta B* **61**, 1129–1134.
- Streli, C., Wobrauschek, P., Meirer, F., and Pepponi, G. (2008). "Synchrotron radiation induced TXRF," *J. Anal. At. Spectrom.* **23**, 792–798.
- Wobrauschek, P. (2007). "Total reflection X-ray fluorescence analysis – a review," *X-ray Spectrom.* **36**, 289–300.
- Wobrauschek, P. and Kregsamer, P. (1989). "Total reflection X-ray fluorescence analysis with polarized X-rays, a compact attachment unit, and high energy X-rays," *Spectrochim. Acta* **44B**, 453–460.
- Wobrauschek, P., Görgl, R., Kregsamer, P., Streli, C., Pahlke, S., Fabry, L., Haller, M., Knöchel, A., and Radtke, M. (1997). "Analysis of Ni on Si-wafer surfaces using synchrotron radiation excited total reflection X-ray fluorescence analysis," *Spectrochim. Acta B* **52**, 901–906.
- Wobrauschek, P., Streli, C., Kregsamer, P., Meirer, F., Jokubonis, C., Markowicz, A., Wegrzynek, D., and Chinea-Cano, E. (2008). "Total reflection X-ray fluorescence attachment module modified for analysis in vacuum," *Spectrochim. Acta B* **63**, 1404–1407.